Comparison of Electron and Neutron Compton Scattering from Entangled Protons in a Solid Polymer

C. A. Chatzidimitriou-Dreismann,[1,*] M. Vos,[2,†] C. Kleiner,[1] and T. Abdul-Redah[3,4,‡]

[1]*Institute of Chemistry, Stranski-Laboratory, Technical University of Berlin, Strasse des 17. Juni 112, D-10623 Berlin, Germany*
[2]*Atomic and Molecular Physics Laboratories, Research School of Physical Sciences and Engineering, The Australian National University, Canberra ACT 0200, Australia*
[3]*Physics Laboratory, The University of Kent at Canterbury, Canterbury, Kent CT2 7NR, United Kingdom*
[4]*ISIS Facility, Rutherford Appleton Laboratory, Didcot, Oxfordshire OX11 0QX, United Kingdom*

(Received 17 January 2003; published 1 August 2003)

We present, for the first time, a direct comparison between electron (ECS) and neutron (NCS) Compton scattering results from protons of a solid polymer. The momentum distributions of hydrogen obtained from ECS and NCS are in excellent agreement. In both experiments, a strong "anomalous" shortfall in the scattering intensity of protons {first detected in liquid water with NCS [C. A. Chatzidimitriou-Dreismann *et al.*, Phys. Rev. Lett. **79**, 2839 (1997)]} is found ranging from about 20% up to 50%, depending on the momentum transfer applied. The characteristic times of electron- and neutron-proton collisions lie in the subfemtosecond range. The presented ECS and NCS results provide further direct evidence for this striking effect, which has been ascribed to attosecond quantum entanglement of the protons.

DOI: 10.1103/PhysRevLett.91.057403 PACS numbers: 78.70.–g, 03.65.Ud, 61.12.–q, 61.14.–x

A large number of experiments have confirmed the existence of quantum entanglement (QE) in an impressive way. QE is the focus of several developing theoretical [1], experimental, and technological fields [2]. In condensed matter, QE of massive particles is able to survive only for very short times [3]. In Ref. [4], we were able to demonstrate such QE with the aid of neutron scattering experiments at sufficiently high momentum transfers ($\hbar\mathbf{q}$).

Usually, however, such high-q experimental techniques are applied to measure momentum distributions of target particles. The basic principles are rather simple. The momentum transfer $\hbar\mathbf{q}$ is such that $1/|\mathbf{q}|$ is much smaller than the atomic dimensions. In that case the probing particle scatters from a single target particle, and one determines $\hbar\mathbf{q}$, and the energy transfer ε, from the probing particle to the target particle. If the target particle (mass m) was moving before the collision with momentum $\hbar\mathbf{k}$, momentum and energy conservation dictates that ε is given by $\varepsilon = (\hbar q)^2/(2m) + \hbar^2\mathbf{k}\cdot\mathbf{q}/m$. This simple physical context has been used to study the momenta of nucleons in nuclei using high energy electrons [5] or protons [6] as probing particles, electron momentum distribution in atoms, molecules, and solids [7,8], using photons or electrons as the probe, and the momentum distribution of nuclei in condensed matter, using epithermal neutrons as probing particles [4,9–14]. The latter technique — named neutron Compton scattering (NCS) — needs large fluences of epithermal neutrons and thus is practical only with spallation sources such as the ISIS facility, United Kingdom. During the past decade, NCS has been established as an experimental method of broad applicability, particularly for studies of proton dynamics and momentum distributions in a great variety of materials.

Recently, using an electron spectrometer with an improved energy analyzer [15], Vos [16] observed electron Compton scattering (ECS) from protons. Using electrons with energies 15–30 keV, Compton recoil from protons of C-H bonds of a solid polymer has been observed. This instrument achieves electron-proton energy transfers in the range of about 2–12 eV, and an energy resolution better than 0.4 eV. The energy loss spectra obtained show that the recoil peak of H is well resolved from the combined peak of the heavier atoms C and O. In this physical context, the ECS method is the electron analog to NCS. We emphasize that, throughout this Letter, the abbreviation ECS always refers to *electron-nucleus scattering* only, and not to electron-electron scattering.

In this Letter, we compare ECS and NCS investigations using a solid polymer known as formvar ($C_8H_{14}O_2$), an amorphous polymer widely used in electron microscopy since it makes extremely thin and flexible films. It also contains no double bonds, which would produce additional peaks in the energy loss spectra (cf. Fig. 1), thus obscuring the ECS peak of H. The combined results, obtained at $T \approx 295$ K, demonstrate (i) the ECS technique provides proton momentum distributions which are in quantitative agreement with those obtained with NCS (cf. Fig. 2). (ii) The striking phenomenon given by the shortfall of scattering intensity from protons, first revealed with NCS from water [4], is observable also with ECS, and the observed anomaly has roughly the same magnitude in both experiments (cf. Fig. 4).

The ECS results were obtained with the electron spectrometer [15,16] of the Australian National University at Canberra. Various thin films of formvar (about 50–100 Å thick) were prepared by standard procedures. The impinging electrons have kinetic energies from 15 to 30 keV;

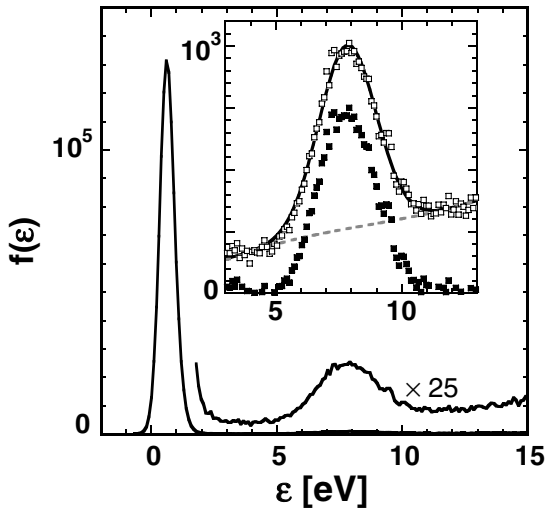

FIG. 1. ECS spectrum of a formvar film taken using 25 keV electrons, thus effectuating a momentum transfer $\hbar q$ with $q = 61.8$ Å^{-1}. The main peak at $\varepsilon = 0.6$ eV energy loss is due to electrons scattered from C and O. The small peak near 8 eV is due to electrons scattered from protons. Inset: The fit of the peak related to proton recoils (open symbols) with a Gaussian and a quadratic background (broken line) is shown by the full line.

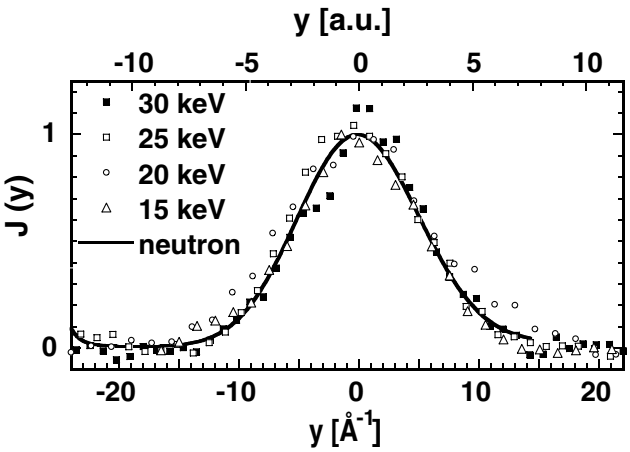

FIG. 2. Distributions $J(y)$ derived from the ECS and NCS measurements, with $\hbar y$ being the H-momentum component (before collision) along the direction of momentum transfer $\hbar\mathbf{q}$. The abscissa is given in Å^{-1} and in atomic units (a.u., on the top). The scatter in the four ECS measurements (energies as indicated, individual symbols) is an indication of the statistical errors. The graph given by the full line represents $J(y)$ derived with NCS at scattering angle $\theta = 66°$. NCS results at different angles are similar. For comparison, all distributions are normalized to have the maximum about 1. Note that all distributions derived by ECS and NCS have similar widths and shapes.

transmitted electrons are detected at an angle of $\theta = 44.3°$ in the forward scattering direction. These experiments provided results which confirmed and extended the previous findings reported in Ref. [16]. An ECS spectrum $f(\varepsilon)$, where ε is the energy transfer, is shown in Fig. 1, together with the corresponding fit. As is done in NCS investigations [11], the electron spectra $f(\varepsilon)$ are fitted with Gaussians. For the baselines, various quadratic and higher-order polynomial fits have been performed. The "background" of the peaks is mainly due to interactions of the incident electrons with electrons in the sample. It was found that the results (see below) depend only slightly on the different fitted baselines.

From these measured ECS profiles, momentum distributions of protons are derived. The magnitude of the electron momentum $\hbar k$ remains almost constant (since ε is much smaller than the kinetic energy of the impinging electrons). Note that this approximation is not valid for NCS. In Fig. 2, we show the four measured distributions $J(y)$ (often called "Compton profiles," see Section 3 of Ref. [11]) as obtained from ECS using electrons of 15, 20, 25, and 30 keV. (These energies correspond to q values of about 47.6, 55.1, 61.8, and 67.8 Å^{-1}, respectively.) $J(y)$ is proportional to the density of protons with momentum component $\hbar y$ along the direction of the electron-proton momentum transfer $\hbar\mathbf{q}$. For comparison, these data are presented together with the corresponding distribution derived from a NCS time-of-flight (TOF) spectrum.

The NCS experiments were carried out at ISIS with VESUVIO (formerly eVS), an "electron volt spectrometer" [11–14,19]. The filter-difference method [19] was used, with a gold absorber. It absorbs neutrons at 4.908 eV, with a resonance width of about 0.28 eV. Various self-supporting foils of formvar (typically 0.1–0.2 mm thick) were prepared by standard procedures. The 32 neutron detectors used cover an angular range of 32° to 68°, which, for neutron-proton scattering, corresponds to a range of q values of about 30–120 Å^{-1} and of energy transfers $\varepsilon \approx 2$–30 eV. Figure 3 shows a measured TOF spectrum together with the corresponding fit (for the data analysis procedure, see, e.g., [11–14,17,18]). Here it suffices to mention that the analysis software also takes into account so-called "final state effects," which are due to the fact that the impulse approximation is exact only when q and ε are infinite [10–12].

The momentum distributions of H and other atoms are derived from the measured TOF spectra by standard procedures [12,13]. The distribution $J(y)$ of H derived from the NCS data at scattering angle $\theta = 66°$ is shown in Fig. 2. The agreement, within experimental errors, between the graphs shown, confirms that all these measurements reveal the same physical quantity: the (projection on the scattering vector $\mathbf{q}$ of the) momentum density distribution of the protons of the sample. The electron and neutron results of Fig. 2 can be compared directly as the experimental energy resolution contributes a negligible amount to the width of the spectra obtained by either technique.

We now shortly discuss the observed decrease of NCS intensity from H [4], which is represented by the violation of the basic equation $R_{\text{exp}} = R_{ia}$ (see below). Because of

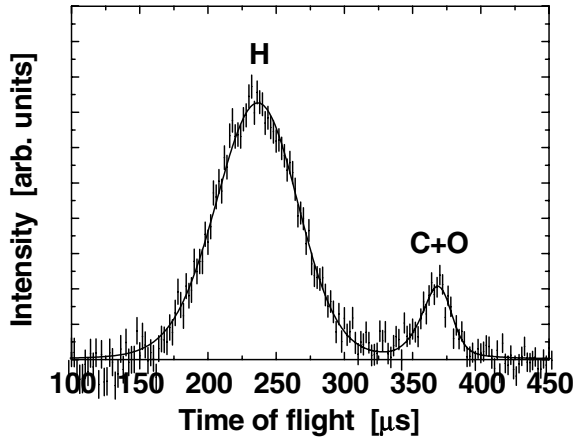

FIG. 3. Example of a measured TOF spectrum by NCS of formvar (self-supporting foil, 0.1 mm thick), with the associated fit (line). The spectrum is taken with the detector at scattering angle $\theta = 51.27°$, which corresponds to a mean momentum transfer (for the neutron-proton collision) with $q \approx 60.7$ Å^{-1}. The broad H peak is well resolved from the narrow recoil peak from C and O. The ratio of peak areas R_{exp} is about 40% lower than the conventionally expected value R_{ia}; cf. Equations (1) and (2).

the large momentum and energy transfers involved in NCS, the recoil peaks of protons are well resolved from those of C and O (which overlap, cf. Fig. 3) in the TOF spectra [20]. From a measured TOF spectrum, the data analysis procedure [13] determines the double differential cross section $d^2\sigma/d\varepsilon d\Omega$, which is proportional to the *bound* total cross sections σ_X for each scattering atom X, cf. [21]. Thus, the peak areas A_X (with $X = \mathrm{H}$, C, O) extracted from $d^2\sigma/d\varepsilon d\Omega$ are proportional to σ_X [4,13,17]. From the experimental data, one thus determines the ratio

$$R_{\mathrm{exp}} \equiv A_{\mathrm{H}}/(A_{\mathrm{C}} + A_{\mathrm{O}}). \tag{1}$$

If the so-called "incoherent approximation" [10,11] is assumed (which means that each deflected neutron is scattered from an individual nucleus), the expected value R_{ia} of this ratio is calculated with (cf. [4])

$$R_{ia} = N_{\mathrm{H}}\sigma_{\mathrm{H}}/(N_{\mathrm{C}}\sigma_{\mathrm{C}} + N_{\mathrm{O}}\sigma_{\mathrm{O}}). \tag{2}$$

($\sigma_{\mathrm{H}} = 82.02$ b, $\sigma_{\mathrm{C}} = 5.551$ b, $\sigma_{\mathrm{O}} = 4.232$ b, 1 b $= 10^{-24}$ cm^2; cf. [21]). N_X is the number density of atom X (= H, C, O), which is for formvar N_{H}:N_{C}:$N_{\mathrm{O}} = 14$:8:2. Instead of the expected equality $R_{\mathrm{exp}} = R_{ia}$, however, the experimental results presented below show that R_{exp} is considerably smaller than R_{ia}. This effect has been observed by NCS in a great variety of liquid and solid materials since 1995; cf. [4,17,18].

For the same physical reasons, equality $R_{\mathrm{exp}} = R_{ia}$ should be valid for ECS also. Here, the cross section for electron scattering from hydrogen, carbon, and oxygen is simply the Rutherford cross section: $\sigma_X \propto Z_X^2$ (Z_X: atomic number of atom X). Calculations of the cross section based on the electronic structure show that screening effects are not important under these conditions [22]. In agreement with preliminary observations [16], the following results show that the ratio R_{exp} of the hydrogen peak and the joint oxygen/carbon peak is decreased, too.

In Fig. 4, the ratios R_{exp}/R_{ia} are given as functions of $q = |\mathbf{q}|$ for both ECS and NCS. The effect revealed by NCS is between 25% and 50%, and increases with increasing momentum transfer, corresponding to decreasing scattering time τ_{sc} (see below). The ECS data reveal a corresponding anomaly of R_{exp} of 15%–45%. The associated systematic and statistical errors of the ECS results (including the uncertainty of the baseline of the H peak) are estimated to be about $\pm 10\%$. For the ECS experiment, it was checked that no radiation induced modifications of the film occurred for doses required to obtain good quality spectra [23]. Considerable efforts to identify various possible sources of NCS-experimental errors have been made; see, e.g., Refs. [17b,17c]. In particular, the constancy of NCS results by doubling the thickness of the formvar foil, as shown in Fig. 4, shows that multiple scattering effects are very small.

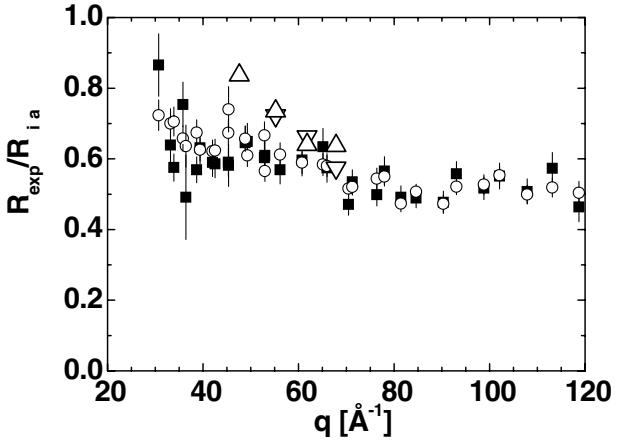

FIG. 4. Anomalous reduction of scattering intensity from H of formvar, as a function of applied momentum transfer $\hbar q$ (with $q = |\mathbf{q}|$); cf. Equations (1) and (2). The q range shown corresponds to scattering times $\tau_{sc} \approx 300$–1000×10^{-18} s. Squares, circles: Values of R_{exp} of NCS spectrum areas (for 32 detectors in the angular range about 32°–68°), relative to R_{ia}, Eq. (2). Full squares represent results for $t = 0.1$ mm formvar foils, open circles those for $t = 0.2$ mm. They are equal within experimental errors, indicating that multiple scattering effects are insignificant. Large open triangles: R_{exp}/R_{ia} as measured by ECS from formvar films of 50–100 Å thickness, for electrons with kinetic energies 15–30 keV. (The overall errors of these results are estimated to be about 10%, see the text.) The results demonstrate a strong (20–50%) shortfall of scattering intensity from H, which is q dependent. Note that the ECS value at $q = 47.6$ Å^{-1} may be larger than the corresponding NCS value. ECS also provides a new confirmation (independent from NCS) of the considered QE effect [4,17,18].

These results demonstrate that the effect of decreased NCS intensity from protons [4,17,18] is also observable with a considerably different method, i.e., ECS. This is important, as this effect appears to be independent of the two fundamental interactions involved (i.e., electromagnetic versus strong interaction).

This effect (in the context of NCS) has been theoretically expected [4] and ascribed to short-lived protonic quantum entanglement, also involving "dressing" with electronic degrees of freedom; for various theoretical discussions cf. Refs. [17,24,25]. In this connection it should be also mentioned that, in a good approximation, the expected scattering times τ_{sc} of ECS and NCS — i.e., the duration of the interaction time of the electron/neutron with a proton — may be assumed to be similar. This appears to be justified since both methods are based on the basic physics of Compton scattering, and since the energy and momentum transfers applied are similar. According to basic NCS theory [10,11], it holds: $\tau_{sc} v_0 q \approx 1$, where v_0 is the root-mean-square velocity of the proton in its state before collision and $\hbar q$ is the magnitude of the momentum transfer. These scattering times lie in the attosecond range, i.e., about 300–1000 $\times$ 10^{-18} s cf. [17,18,24]. This also implies that, under the physical conditions of ECS and NCS, there is no well-defined time scale separation between electronic and nuclear (protonic) motion — which obviously implies that the widely used theoretical concept of electronic Born-Oppenheimer energy surfaces is not applicable here.

In conclusion, we demonstrated that ECS analysis of the H-recoil peak taken at large momentum transfer reveals to a considerable extent the same information as NCS. Moreover, and perhaps more importantly, the ECS technique has been shown to provide an additional (complementary to NCS) tool for the experimental investigation of the striking anomalous shortfall of scattering intensity of protons and the associated attosecond entanglement in condensed matter.

We thank J. Mayers for close collaboration and ISIS for providing beam time. This work was partially supported by the Australian-German (DAAD) Joint Research Cooperation Scheme. C. A. C.-D. acknowledges helpful discussions with E. B. Karlsson and support, in part, by the Fonds der Chemischen Industrie, the EU network QUACS, and a grant from the Royal Swedish Academy of Sciences.

*Electronic address: dreismann@chem.tu-berlin.de
†Electronic address: maarten.vos@rsphysse.anu.edu.au
‡Electronic address: t.abdul-redah@rl.ac.uk

[1] See, e.g., M. A. Nielsen and I. L. Chuang, *Quantum Computation and Quantum Information* (Cambridge University Press, Cambridge, England, 2000).
[2] See, e.g., *Foundations of Quantum Mechanics in the Light of New Technology, ISQM–Tokyo'01*, edited by Y. A. Ono and K. Fujikawa (World Scientific, New Jersey, 2002).
[3] W. H. Zurek, Rev. Mod. Phys. **75**, 715 (2003).
[4] C. A. Chatzidimitriou-Dreismann, T. Abdul-Redah, R. M. F. Streffer, and J. Mayers, Phys. Rev. Lett. **79**, 2839 (1997).
[5] I. Sick, D. Day, and J. S. McCarthy, Phys. Rev. Lett. **45**, 871 (1980).
[6] A. E. L. Dieperink and T. De Forest, Jr., Annu. Rev. Nucl. Sci. **25**, 1 (1975).
[7] *Compton Scattering: The Investigation of Electron Momentum Distributions*, edited by B. G. Williams (McGraw-Hill, New York, 1977).
[8] M. Cooper, Rep. Prog. Phys. **48**, 415 (1985).
[9] P. C. Hohenberg and P. M. Platzman, Phys. Rev. **152**, 198 (1966).
[10] V. F. Sears, Phys. Rev. B **30**, 44 (1984).
[11] G. I. Watson, J. Phys. Condens. Matter **8**, 5955 (1996).
[12] J. Mayers, Phys. Rev. Lett. **71**, 1553 (1993).
[13] J. Mayers, T. M. Burke, and R. J. Newport, J. Phys. Condens. Matter **6**, 641 (1994), Sect. 2.
[14] G. F. Reiter, J. Mayers, and P. Platzman, Phys. Rev. Lett. **89**, 135505 (2002).
[15] M. Vos, G. Cornish, and E. Weigold, Rev. Sci. Instrum. **71**, 3831 (2000).
[16] M. Vos, Phys. Rev. A **65**, 012703 (2002).
[17] (a) C. A. Chatzidimitriou-Dreismann, T. Abdul-Redah, and B. Kolarić, J. Am. Chem. Soc. **123**, 11 945 (2001); (b) C. A. Chatzidimitriou-Dreismann, T. Abdul-Redah, R. M. F. Streffer, and J. Mayers, J. Chem. Phys. **116**, 1511 (2002); (c) C. A. Chatzidimitriou-Dreismann, T. Abdul-Redah, and J. Mayers, Physica (Amsterdam) **315B**, 281 (2002).
[18] (a) E. B. Karlsson *et al.*, Europhys. Lett. **46**, 617 (1999); (b) T. Abdul-Redah *et al.*, Physica (Amsterdam) **276B–278B**, 824 (2000).
[19] R. M. Brugger, A. D. Taylor, C. E. Olsen, J. A. Goldstone, and A. K. Soper, Nucl. Instrum. Methods **221**, 393 (1984).
[20] It is worth noting that the areas of the peaks in a TOF spectrum are — among other quantities cf. [13] — proportional to the product of the *free* total cross sections σ_X^{free} and a function of θ and m_n/m_X; cf. [21b], Eq. (1.88) [m_n: neutron mass; m_X: mass of atom X]. σ_X^{free} are related to the conventionally tabulated *bound* total cross sections σ_X by $\sigma_X = \sigma_X^{\text{free}}(1 + m_n/m_X)^2$ [21].
[21] (a) G. L. Squires, *Introduction to the Theory of Thermal Neutron Scattering* (Dover, Mineola, 1996); (b) S. W. Lovesey, *Theory of Neutron Scattering from Condensed Matter* (Clarendon, Oxford, 1984).
[22] M. E. Riley, C. J. MacCallum, and F. Biggs, At. Data Nucl. Data Tables **15**, 443 (1975).
[23] M. Vos, Ultramicroscopy **92**, 143 (2002).
[24] (a) E. B. Karlsson and S. W. Lovesey, Phys. Rev. A **61**, 062714 (2000); Phys. Scr. **65**, 112 (2002); (b) E. B. Karlsson, Phys. Rev. Lett. **90**, 095301 (2003).
[25] C. A. Chatzidimitriou-Dreismann, J. Alloys Compd. **356C–357C**, 244 (2003).